0.1 Transition from Spiking to Bursting

0.1.1 EAG channel expression modulates spiking-bursting transition

As it was discussed in Section **??**, one possible mechanism behind the transition of R5 activity between tonic firing and bursting may be due to diurnal variation in expression of the ether-à-go-go (EAG) channel. EAG is permeable to potassium. During the night, expression of these channels is low compared to the day. As potassium current is hyperpolarizing, increased expression of EAG channels during the day might potentially decrease excitability of the cell and thus, the number of spikes per burst.

EAG channels are voltage-gated ion channels. The family of EAG channels contains several subtypes. Some of them are inactivating (i.e. contain an inactivation gate), while others are non-inactivating (i.e. lack an inactivation gate) (Bauer and Schwarz 2018). The kinetic properties of these channels in *Drosophila* are not extensively documented in the literature. I could find only a single paper providing kinetic properties of these channels in *Drosophila* (Bronk et al. 2018). Although the original model of the EAG channel described in the paper is blocked by Ca^{2+}, the present work assumes that the gating mechanism depends solely only on membrane potential, for simplicity. This simplification is justified for several reasons. First, the EAG channels are generally considered to be voltage-gated (Bauer and Schwarz 2018). Second, to my knowledge, the exact biophysical properties of these channels have not been characterized in R5 neurons - only the expression of the gene encoding the channel has been identified in these cells (Dopp et al. 2024). Third, in the model proposed by Bronk and Schwarz, EAG channels are inactivated by calcium. However, for these channels to contribute to burst termination, the calcium-dependent inactivation must be either weak or sufficiently slow. Otherwise, calcium influx during a burst would prevent it from contributing to burst termination. Therefore, calcium-dependent inactivation of EAG channels is unlikely to play a significant role in the transition from bursting to spiking in R5 neurons.

In the literature, bursting models generally lack EAG channels. Thus, I added the channel to the Wang model to test the above-mentioned hypothesis. The parameters for EAG channel were adapted from (Bronk et al. 2018), with few modifications that will be discussed below. The current through the channel was added to the total ionic current $\sum I_{\text{ion}}$ in Equation **??** and

is governed by:

$$I_{\text{EAG}} = g_{\text{EAG}} m^2 (V - V_K) \tag{0.1}$$

where g_{EAG} is the conductance, V_K is reversal potential of potassium, and m is activation variable governed by Equation **??**. The voltage is measured in millivolts, while the maximal conductance and current are expressed in either mS/cm^2, or S/cm^2 and $\mu A/cm^2$ or mA/cm^2, respectively, depending on the model (Appendix **??**). The steady state activation $m_\infty(V)$, and activation time constant $\tau(V)$ are governed by:

$$m_\infty(V) = \left(\frac{1}{1 + \exp\left(-(V + 23.12 - d)/k\right)} \right) \tag{0.2}$$

$$\tau(V) = a \left(5497 - \frac{5500}{1 + \exp((V + 251.5 - d)/(-16.94 - 51.5))} \right) \tag{0.3}$$

Note that Equation 0.2 lacks dependency on calcium, in contrast to the one proposed in (Bronk et al. 2018). Equation 0.2, is a sigmoid function, where the parameter K^+ determines the slope of the sigmoid and was set to 16.94 in (Bronk et al. 2018). The parameter d, measured in millivolts, was introduced into the model to allow a voltage shift in the steady-state activation function $m_\infty(V)$ and the gating time constant $\tau(V)$. Since different models operate over slightly different membrane potential ranges, d serves to adjust the voltage range in which the ion channel is active. The parameter a, which is unitless, was introduced to scale the activation time constant. It modulates the rate at which the gating variable converges to its steady-state value at a given membrane potential.

To investigate whether the EAG channel can affect the number of spikes per burst, the parameters d and a were manually tuned such that the addition of the channel did not alter the oscillation period. This constraint was particularly important for the Wang model, as it is fragile with respect to perturbations in external current - small changes in input dramatically affect the oscillation period (Wang 1994). In general, if the added ion channel conducts current at membrane potentials between bursts, the hyperpolarizing nature of the EAG current can counteract the depolarizing currents and delay the membrane potential from reaching the spiking threshold, thereby extending the oscillation period.

Note that this is a strong condition, motivated by literature reporting tonic firing of R5 neu-

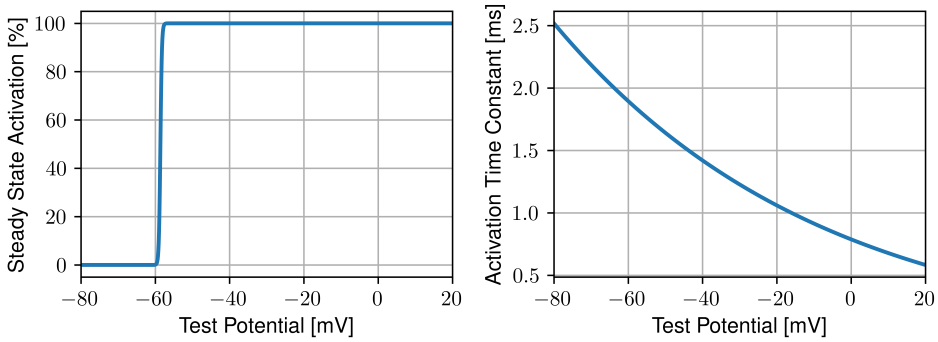

Figure 1: EAG Channel Activation Variable and Kinetics for the Wang Model. Steady state activation function (left) and activation time constant (right) of EAG channel following parameter adjustement. For the original values see Figure **??** and Table **??**.

rons during the daytime. However, further data analysis is needed, and it is possible that the assumption of tonic firing - and thus the above-mentioned requirement - may need to be revised see Discussion in Section **??**. Additionally, the frequency of the tonic spiking is lower than the frequency of bursting observed in R5 neurons (Figures **??** and **??**). Apart from variations in synaptic input from other neurons, the difference in frequency could potentially result from the variation in the expression of the EAG channels between day and night.

Table **??** provides the exact parameter values used in the simulations. Figures 1 and **??** illustrate Equations 0.2 and 0.3, showing their dependence on membrane potential for parameter sets corresponding to different models (see also Figure **??** for the default parameters provided in (Bronk et al. 2018)).

To investigate the transition between tonic spiking and bursting mediated by the EAG channel, g_{EAG} in Equation 0.1 was varied from 0 to 1 mS/cm^2 to reflect potential changes in channel expression between day and night (note that maximal conductance reflects the number of ion channels in the conductance based model). To account for variations in the external input during the day and night, the external current was also varied. All other parameters were set to their default values as specified in Appendix **??**. Figure 2 shows how the activity, interburst interval, and number of spikes per burst depend on g_{EAG} and external current for the model of thalamic relay neuron proposed by Wang (Wang 1994). Activity is classified as bursting, spiking, or resting and was determined as described in Section **??**. For the purposes of analyzing interburst interval and spike count, tonic spiking was treated as a special case of bursting, consisting of one spike per burst.

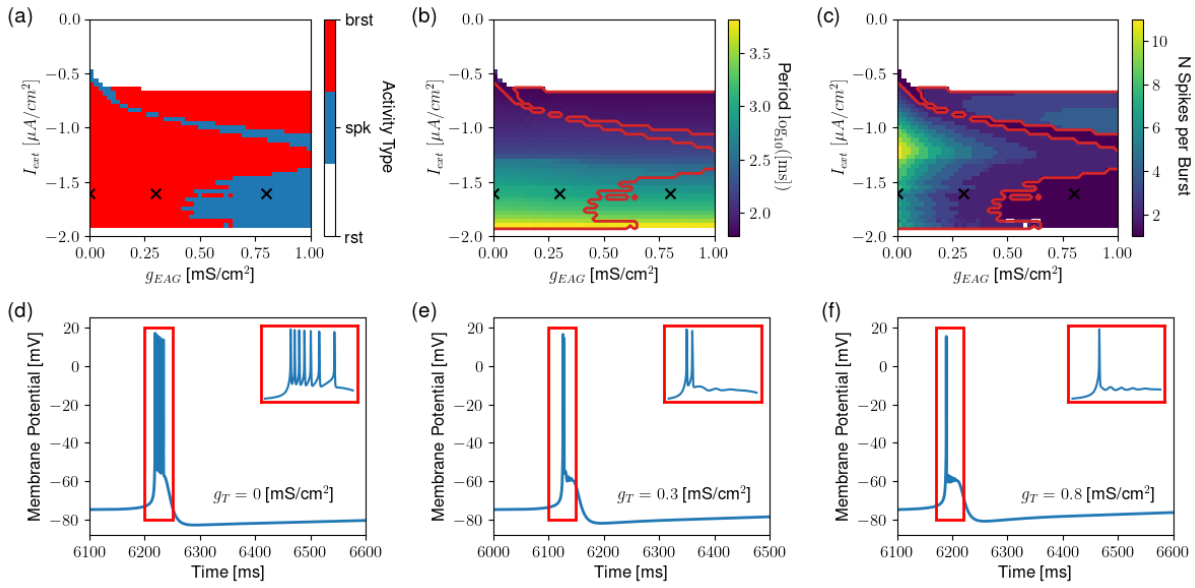

Figure 2: Spiking-to-Bursting Transition Induced by EAG Channels in Wang model. Thy x axis indicates the maximal conductance of the EAG channels, and the y axis shows the magnitude of the constant external input. Simulations were done for combinations of the input current and g_{EAG} within the illustrated parameter range. (a) Activity type, classified as bursting (red), spiking (blue), or resting (white) (see the details about classification in Section **??**); (b) Oscillation period of bursting or spiking; (c) Number of spikes per burst. Within this context, bursting is referred to as activity when the neuron exhibits at lest two spikes per burst. Region where the model neuron exhibitied bursting activity is indicated by the red contour. Here, tonic spiking can be thought of as one spike per burst; (d-f) The representative voltage traces for different parameter regimes indicated by the "x" markers in Figures (a-c). The inset plots show zoomed version of bursts, as indicated by the red rectangles. The number os pikes per burst decreases with increasing g_{eag} withoug considerable effect on the period.

For fixed external input, the number of spikes mainly decreases with increasing g_{EAG} and the firing pattern switches from bursting to tonic firing for a critical value of g_{EAG}, while the period remains relatively constant (Figure 2a-c). Figures 2d-f further illustrate this effect by showing voltage traces from three representative simulations. The corresponding parameter combinations are indicated by 'x' in Figures 2a-c. Interestingly, there is a region in the phase space where the number of spikes increases with increasing g_{EAG} (Figure 2c, upper boundary). However, closer look indicated that these region corresponded to the low-amplitude oscillations (Figures **??** and **??**). Therefore, this region is not of interest.

0.1.2 Bifurcation analysis

In the previous section, it was demonstrated that the EAG channel may be responsible for termination of the burst and the emergence of tonic spiking–like behaviour in R5 neurons. This section investigates the underlying mechanisms through bifurcation analysis.

Figure 3 presents the results of the bifurcation analysis for the extended Wang model with the added EAG channel. The original model generates bursting behaviour mediated by T-type Ca^{2+} channels. In the model proposed by Wang (Wang 1994), the activation gate of the T-type channel is treated as instantaneous (see Appendix **??** for details), and the slow dynamics are governed by the inactivation gate, denoted by the variable h. To investigate how bursting depends on this variable, h was treated as a bifurcation parameter, while all other variables were allowed to evolve freely.

The analysis was performed for three representative values of g_{EAG} corresponding to the 'x' markers in Figure 2a-c. For each value of h, the stable and unstable fixed points were computed using AUTO-07P, along with the locations of Hopf and saddle-node (Saddle-Node (SN)) bifurcations. In Figure 3, stable and unstable fixed points of the reduced system (i.e. when variable h is treated as a constant) are shown as solid and dashed black lines, respectively. Hopf bifurcations are indicated by circles, and saddle-node bifurcations by triangles. Periodic orbits were numerically continued from the Hopf bifurcations. The bursting trajectory was obtained by numerical simulations of the full system. Projection of the trajectory on the V-h plane is overlaid as a green curve. The direction of the trajectory is indicated by the black arrows at the bottom of the plots.

The analysis is similar to the fast-slow decomposition discussed in Section **??**. Note that plots in Figure 3 extend to negative values of h. Although $h < 0$ values do not have a physiological meaning, they are important for the completeness of the mathematical analysis.

EAG channel can mediate the transition from spiking to resting state

Let us first focus on the state in which the system is spiking. In the absence of EAG channels ($g_{\text{EAG}} = 0$, Figure 3 left), the trajectory is attracted by the stable limit cycle after the resting state of the reduced system (i.e. one without the h variable) loses stability, causing transition of the system to the spiking state (stable limit cycle (LC), solid red lines). In the spiking state, the

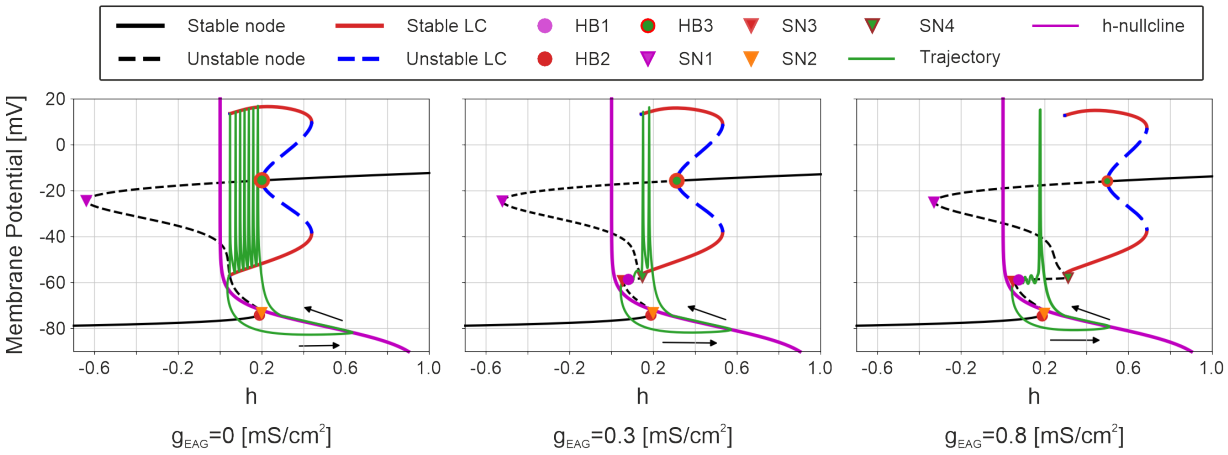

Figure 3: Transition from Spiking to Bursting via EAG channels. Figure shows bifurcation diagram following fast-slow decomposition of the extended Wang model, for different values of the maximal conductance of the EAG channels. The slow variable h corresponds to the inactivation gate of T-type calcium channels. Left: In the absence of the EAG channel, once the trajectory is attracted by the limit cycle, the fast subsystem induces negative feedback to the slow variable. After several spikes the limt cycle collides with unstable fixed point of the fast subsystem and looses stability. Trajectory returns to the resting state and the cycle repeats. Middle: With increasing g_{EAG}, the upper part of the nullcline shifts to the right, while the point where the transition from spiking to resting state occurs remain unaffected. Consequently, the system spends less time in the LC regime, thereby reducing number of spikes per burst; (right) after some critical value of g_{EAG} the system is not attracted by the LC anymore. The spike, however, is still observed due to heteroclinic orbit.

membrane potential provides a negative feedback to the variable h, corresponding to the inactivation of the corresponding gate. Consequently, the trajectory moves to the left of the V-h plane until the stable limit cycle collides with the unstable fixed point of the reduced system. This is commonly referred to as saddle-homoclinic orbit bifurcation (Izhikevich 2006; Izhikevich 2000) (see also Section **??**).

When g_{EAG} is increased, the upper curve of the V-h nullcline (black curve) is shifted to the right. This causes the saddle-homoclinic bifurcation to occur for higher values of h. Consequently, the system spends less time in the spiking state with increasing value of g_{EAG}, resulting in fewer spikes per burst (Figure 3, middle).

After g_{EAG} reaches a critical point (the exact value not shown here), the trajectory does not enter the region of the V-h plane where the limit cycle exists. Consequently, after the fixed point of the reduced system loses stability, instead of following a limit-cycle attractor, the trajectory goes back to rest via a heteroclinic orbit (Figure 3 right).

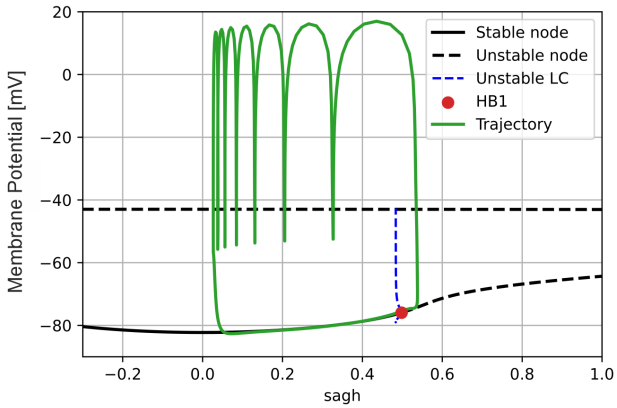

Figure 4: Bifurcation Diagram - Wang Model with Sag Activation as Bifurcation Parameter. Bifurcation diagram of the extended WANG model in case when the activation of the sag (or, h-) current was treated as a slow variable. The figure illustrates, that at rest the trajectory is affected more by the h-current.

Effect of another slow variable on fast-slow decomposition

From the perspective of fast-slow analysis, one might expect the trajectory of the full system to closely follow the manifold of stable fixed points of the reduced (or, fast) subsystem. However, the model contains an additional variable with a relatively slow timescale, associated with the Hyperpolarization-activated Cyclic Nucleotide-gated (HCN) channels (see Appendix **??**). As discussed in Section **??**, HCN channels (referred to as "sag current" in (Wang 1994)) are hyperpolarization-activated channels that mediate depolarizing current, thus, they contribute to dynamics at relatively low values of membrane potential.

Notably, HCN channels contribute less during the spiking state. For example, at -55mV (approximately trough of the oscillation), the steady state activation has a value of ~ 0.12, decreasing to ~ 0.06 at -50mV and to ~ 0.016 at -40mV. Consequently, during the spiking state, the system behaves more like a fast-slow in contrast to the resting state. This may explain why the bifurcation diagram seems to be more accurate in the spiking state than in the resting state of the reduced ("fast") subsystem without the h variable. Indeed, when the activation variable of the HCN channel was treated as a bifurcation parameter, the resulting trajectory closely followed the manifold of stable fixed points in the reduced subsystem where the HCN activation was held constant (Figure 4).

To summarize, the transition of interest is from the spiking to the resting state, as I hypothesize that EAG channels may terminate bursting activity. Since the above analysis effectively captures the dynamics during the spiking state, the approach remains suitable for investigating the mechanism.